**Steel and Composite Structures**, *Vol. 35, No. 5 (2020) 687-699*
DOI: https://doi.org/10.12989/scs.2020.35.5.687


# Design of buckling restrained braces with composite technique

Ramazan Ozcelik*[1], Yagmur Dikiciasik[2a], Kazim B. Civelek[1b], Elif F. Erdil[1c] and Ferhat Erdal[1d]

[1]*Department of Civil Engineering, Akdeniz University, 07058, Antalya, Turkey*
[2]*Department of Civil Engineering, Karamanoglu Mehmetbey University,70100, Karaman, Turkey*

(*Received January 22, 2020, Revised May 7, 2020, Accepted May 21, 2020*)

**Abstract.** This paper focus on the buckling restrained braces (BRBs) with new casing members (CMs). Seven BRBs with CMs consisting of precast concrete modules (PCMs) were tested to investigate the effects of CMs on the cyclic performance of BRBs. The PCMs consisted of plain and reinforced concrete casted into wooden or steel molds than they were located on the core plate (CP) via bolts. There were 14 or 18 PCMs on the CP for each BRBs. The technique of the PCMs for the CM provides that the BRBs can be constructed inside the steel or reinforced concrete (RC) structures. In this way, their applications may be rapid and practical during the application of the retrofitting. The test results indicated that the cyclic performance of the BRBs was dominated by the connection strength and confinement of the PCMs. The BRBs with PCMs wrapped with fiber reinforced polymers (FRPs) sustained stable hysteretic performance up to a CP strain of 2.0 %. This indicates that the new designed BRBs with PCMs were found to be acceptable in terms of cyclic performance. Furthermore, the connection details, isolation materials and their application techniques have been also investigated for the improved BRB design in this study.

**Keywords:** buckling restrained braces; composite member; cyclic test; out-of-plane buckling

## 1. Introduction

Steel braces are a kind of structural members that carry the lateral loads such as wind and earthquake forces. In the areas prone to earthquakes, the brace members are widely used due to their high axial rigidity. It is well known that the tension and compression capacity of braces are not equal and this fact is the one of the biggest challenges in their design. Black *et al.* (1980) has proved that braces yield under large tension forces but they buckled under compressive forces and then their axial load capacity drops suddenly. This results in unstable seismic performance of the steel braced frames. To shift the axial compression capacity of brace members from unstable to stable they should be prevented from buckling. This fact makes the buckling-restrained braces (BRBs) attractive among researchers all over the world. A general 3-dimensional view of the BRBs consists of a core plate (CP) and casing member (CM) can be seen in the Fig. 1. Although the compression capacity of the CP is very limited or negligible, it can be increased by using a proper CM or restraining its buckling. In this case, the CP may yield or buckle in a high buckling mode under compressive demands. Fig. 1 indicates that the BRBs generally consist of numbers of global zones such as the unrestrained elastic zone (Zone-1 and 2), the restrained elastic zone (Zone-3), the restrained plastic zone (Zone-4 and 5). The CP needs to be separated or isolated from the CM by placing an air gap or using isolation material such as rubber, silicon grease, foam, and so on (Fig. 1). Hence, the friction between the CP and the CM results in the additional axial load capacity can be prevented or limited by using the air gap or isolation material. Furthermore, the effect of the poisson ratio may also cause an additional friction between the CP and the CM hence to determine the gap required between them it can be taken as 0.3 and 0.5 for the elastic range and the plastic range, respectively (Uang and Nakashima 2004). The research about the BRBs started with conducting component and sub-assemblage tests in Japan by Uang and Nakashima (2004), Xie (2004) and Uang *et al.* (2004), in Taiwan by Tsai *et al.* (2002, 2004) and in the USA by Black *et al.* (2002). Watanabe *et al.* (1988) conducted the tests on the BRBs with the mortar-infilled square and the rectangular steel tubes to determine the global buckling of the braces. They proposed the Eq. (1) to prevent the BRB from the global buckling.

$$Pe / Py > 1.0 \tag{1}$$

Where $P_e$ is the elastic buckling strength of the CM and $P_y$ is the yield strength of the CP.

Iwata and Kato (2000) conducted tests on the commercially available BRBs in which the CMs were steel

*Corresponding author, Associate Professor
E-mail: rozcelik@akdeniz.edu.tr
[a]Assistant Professor
E-mail: dyagmur@kmu.edu.tr
[b]Ph.D. Student
E-mail: burccivelek@akdeniz.edu.tr
[c]Ph.D. Student
E-mail: eferdil@akdeniz.edu.tr
[d]Associate Professor
E-mail: eferhat@akdeniz.edu.tr


http://www.techno-press.org/?journal=scs&subpage=8 ISSN: 1229-9367 (Print), 1598-6233 (Online)

tubes filled with mortar and structural steel members. The BRBs with low yield-point steel and a ductile CP were tested by Chen *et al.* (2001). They aimed to avoid the friction between the CP and the CM by using silicone grease. Due to insufficient gap between them, the compression capacity of the BRBs was found to be about 1.5 times higher than their tension capacity. Higgins and Newell (2004) used steel pipe filled with a confined non-cohesive material instead of mortar during the design of the BRBs. Young *et al.* (2009) tested the BRBs with the CP consisted of a structural steel I-section. It was observed from this study that the thicknesses of the external tube (CM) governed the hysteretic behavior the BRBs. Takeuchi *et al.* (2012, 2014) studied about the local buckling failure of BRBs with the CM composed of a circular or rectangular steel tube infilled with mortar. They proposed that the local buckling failure of BRBs depend on the mortar thickness and the shape of the CM.

An experimental study about the BRBs with a CM consisting of built-up section was conducted by Eryasar and Topkaya (2010). Tsai *et al.* (2002) performed tests on the BRBs with steel tubes filled with mortar that were used as a retrofit solution for an existing structure. Tremblay *et al.* (2006) performed tests on the BRBs to investigate the effects of the flexure stress on the BRBs, the plastic length of CP, the axial rigidity, and the fatigue life. Park *et al.* (2012) conducted uniaxial and sub-assemblage tests in order to determine the global buckling of the core.

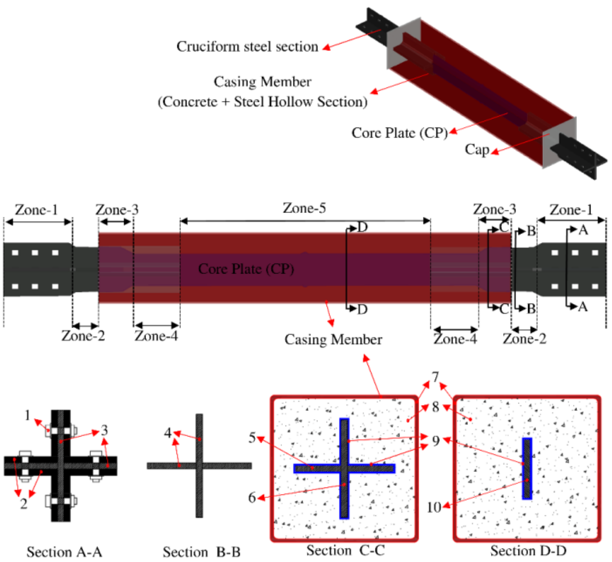


1= Connection bolt, 2= Additional plates, 3 and 4= Cruciform steel section of BRB, 5= Connection plate, 6= Core plate (restrained elastic), 7= Steel hollow section, 8= Concrete (7 and 8 Casing member), 9= Isolation material, 10= Core plate (restrained plastic).

Fig. 1 Three-dimensional view of BRB, zones and cross -sections of BRB

Kim *et al.* (2004) analyzed the steel moment frames with BRB. Razavi *et al.* (2018) conducted a research about the CM consisted of concrete and FRP. Mirtaheri *et al.* (2017), Beiraghi (2017), Beiraghi (2018a), Beiraghi (2018b), Beiraghi (2019) and Maalek *et al.* (2019) simulated the behavior of BRBs by using structural analysis programs. Li *et al.* (2019) studied the FEM of the three-tube buckling-restrained brace which has one core tube and two restraining tubes. Uriz (2005) and Lopez *et al.* (2004) tested the BRBs with concrete-filled tubes in steel frames. Merritt *et al.* (2003) performed sub-assemblage tests on the BRBs using a shake table facility. Hikino *et al.* (2011, 2013) conducted large-scale shake table tests to investigate the out-of-plane stability of BRBs. Kasai *et al.* (2008) performed the test on full-scale five-story buildings with dampers by using three-dimensional shaking table. Five BRB braced frame tests by using static testing methods were conducted by Christopulos (2005). The local buckling of the BRBs occurred during these tests at a drift ratio of 1.5%. Tsai *et al.* (2008) and Tsai and Hsiao (2008) tested on a full-scale three-story three-bay BRB frame by using pseudo-dynamic testing method. Lin *et al.* (2005, 2006) and Tsai *et al.* (2006) investigated the connection between gusset plate and BRBs both experimentally and analytically to prevent the connection failure. Fahnestock *et al.* (2007) conducted tests on a single-bay four-story braced frame by using hybrid dynamic and quasi-static testing procedure. Haydaroglu *et al.* (2011) designed and tested three BRBs with a CM consisted of CFRP retrofitted/wrapped hollow section. Usami *et al.* (2012), Wang *et al.* (2013) and Avci *et al.* (2018) experimentally studied on newly developed BRBs with different core materials (steel and aluminum alloy) and end connection details. Fujishita *et al.* (2015) performed an experimental study to investigate the hysteretic behavior of BRBs with bolted and welded end connections. A simple method in order to predict the cumulative deformation and energy dissipation capacities of BRBs under random amplitudes was proposed by Takeuchi *et al.* (2008). Usami *et al.* (2008) investigated the buckling prevention condition with a series of experiments. Usami *et al.* (2009) conducted tests and analyses to clarify the performance requirements of the BRBs for the damage control seismic design of steel bridges. Chou *et al.* (2016) performed the cyclic tests to compare cyclic performance of dual-core self-centering braces and sandwiched buckling-restrained braces. The columns shared by the orthogonal BRBs to examine the bidirectional loading effects were studied by Sherman and Okazaki (2010). Sabelli *et al.* (2003) analytically examined the seismic response of three and six story concentrically BRB braced frames under the several ground motions to determine the effect of various structural configurations and proportions. Pandikkadavath and Sahoo (2016) analytically studied the hysteretic response of the BRBs with the varying lengths. Mazzolani (2008), Di Sarno and Manfredi (2010, 2012) and Brown *et al.* (2001) examined the seismic retrofitting of deficient reinforced concrete (RC) frames with BRBs. Di Sarno and Elnashai (2008) performed a comparative numerical study to evaluate seismic responses of an existing 9-storey steel moment resisting frames strengthened with several bracing system. Sutcu *et al.* (2014) proposed a simplified method based on an equivalent linearization to design the required amount of BRB and elastic steel frame (SF) capacity to retrofit existing RC buildings. Ozcelik and Erdil (2019) tested three bay-three story deficient RC frame retrofitted by BRBs under several ground motions.

As a result, it is clearly seen that the BRBs with CM consisted of PCMs is absent in the literature. There is need to design a BRB that its application can be conducted inside the existing buildings during the retrofitting (Ozcelik *et al.* 2012). The BRBs in the literature may not be carried inside the building due to their heavy weight. The PCMs enables the BRBs construct inside the existing structures since they can placed on the CP step by step. The weight of the PCMs is between 40 and 60 kg which can be carried without using a forklift or other devices. Therefore, a project has been carried out to investigate innovative CMs and techniques, connection details, and isolation materials for new BRB designs. This paper discusses the different types of CMs, end restrainers, and isolation members.

## 2. Experimental program

The size of the test specimens was determined by considering a full-scale prototype frame. The prototype BRB braced steel frame can be seen in Fig. 2. A column width of 3.5 m and a beam width of 6.0 m were considered for the prototype braced frame. The configurations of BRBs were selected as chevron brace application. Hence, the length of the BRBs was set as 3000 mm.

### *2.1 Test specimens*

The weight of the BRBs tested by Ozcelik *et al.* (2017) and other researchers were about 600-700 kg. Due to unpractical application of heavy BRBs inside the existing buildings, a unit BRB model was designed in this study. This new BRB model was designed in order to present an economical and practical application of the BRBs inside the building without using any construction device.

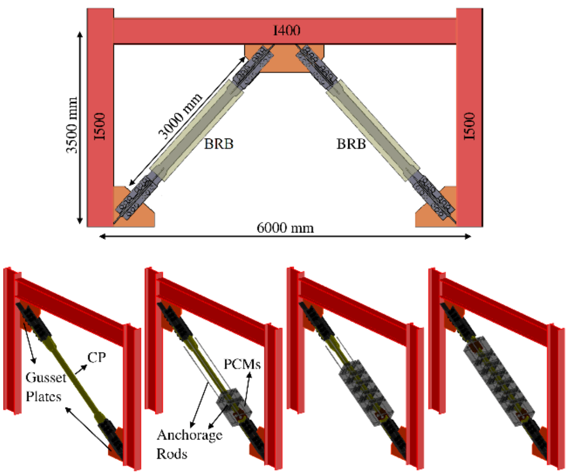


Fig. 2 Prototype frame and assembly steps of PCMs

An experimental research program was conducted on the BRBs with the CM consisted of the PCMs which is suitable for the retrofitting of the existing structures. The technique of the PCMs for the CM provides the BRBs to be constructed inside the structures. In this way, their applications may be rapid and practical during retrofitting. The steps of the application of these BRBs can be summarized as follow: Firstly, the CP is connected to the gusset plate which already fixed to the frame members (Fig. 2). The PCMs are put on the CP step by step and then they are fastened to each other by using longitudinal and vertical rods. Finally, as seen in Fig. 2 the assemblage of BRB is completed.

In order to perform the connection between gusset plate and the BRB the slip-critical connection details given in Eq. (2) is used. Hence, as recommended in the AISC Seismic Provisions (2010), the hole diameter was short-slotted with a width of 27 mm and length 32 mm in the cruciform section of the CP. Thus, the high strength bolts were used for connection between the BRB and the gusset plate.

$$R_n = \mu D_u h_{sc} T_b N \tag{2}$$

Where $R_n$ is the slip-critical strength of a single bolt; $\mu$ is the slip coefficient; $D_u$ equals 1.13 and is a multiplier that reflects the ratio of the mean installed bolt pretension to the specified minimum bolt pretension; $h_{sc}$ is a hole factor; $T_b$ is the specified minimum bolt pretension; and $N_s$ is the number of slip planes.

Seven BRBs were tested in this study. Table 1 summarizes the details of the test specimens. The target 28-day cylinder compressive strength of the concrete used for PCMs was 20 MPa for all BRBs. As given by Eq. (1), the CM should be designed to provide sufficient stiffness to prevent the global buckling of the BRBs. Figs. 3-5 indicate the details of the BRBs application. The low-yield strength steel plate was used for the CP. In the restrained plastic zone, the cross-section of the CP was 15 × 150 mm (2250 mm$^2$) (Zone 4 and 5 in Fig. 1 and Section C-C in Fig. 3). As shown in section B-B in Fig. 3, the restrained elastic zone was designed as cruciform section to facilitate the connection and its cross-section was 6375 mm$^2$. The unrestrained elastic zone had a cross-sectional area of 7875 mm$^2$ as seen in section A-A in Figs. 3 and 4(b). The cross-section of the CP was widened to 3120 mm$^2$ at the mid-span of BRB to prevent the relative displacement between CM and CP (Fig. 4(c)). An air gap was provided instead of isolation material for all BRB members. The test parameters can be summarized as the PCMs consisted of plain concrete (PC), reinforced concrete (RC), reinforced concrete with FRP (Table 1 and Fig. 3). Hence, the details of the test specimen are as follows (Figs. 3-5):

BRB1: The CM consisted of PCMs with the cross-section of 170 x 170 mm (Figs. 3-4(g)-4(n)). The length of the PCMs was designed with respect to their connection type and weight. This means that the length of the PCMs at the both ends of the BRBs is larger than that of PCMs at the middle (Fig. 3). The PCMs was plain concrete hence there was no reinforcement in them. First of all, the wooden molds were prepared then the concrete was casted in the molds (Figs. 4(d)-4(f)). The CP was connected to the gusset

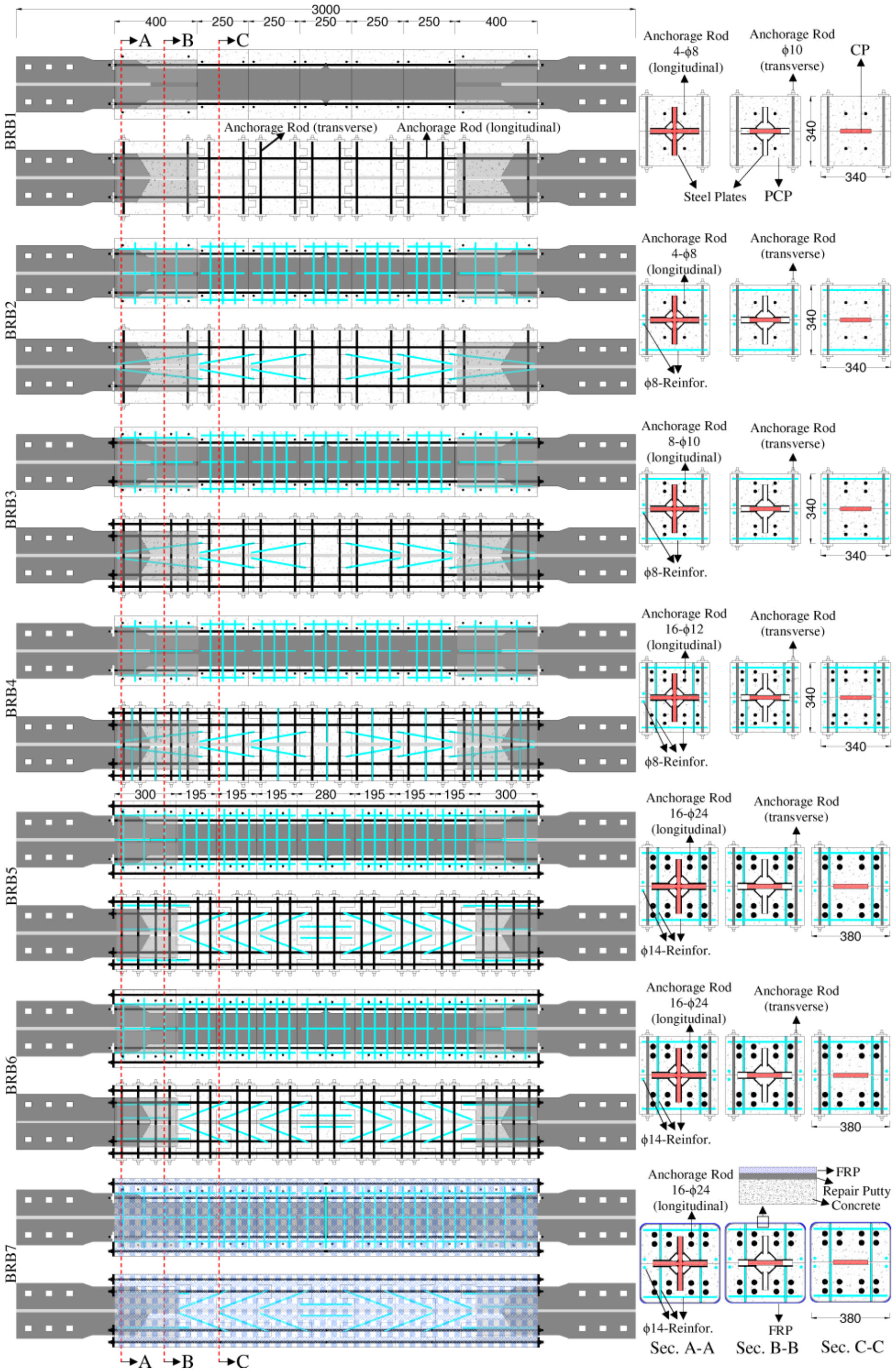

Fig. 3 Test specimens BRB1 to BRB7

plates which already fixed to the frame (Figs. 2-4(i)-4(j)). After curing of the PCMs (Figs. 4(g)-(h)), they were placed on the CP and then they were connected to each other by using the transverse anchorage rods (4ϕ10 for each PCM) and the longitudinal anchorage rods (4ϕ8) (Figs. 3-4(k)-4(n)). There was no de-bonding material such as rubber between CP and CM instead an air gap was provided to prevent the excessive friction between them.

At the both ends of BRB, the PCMs have 400 mm-steel plates (similar details from Ozcelik *et al.* 2017) used as an end restraining system to increase local stability (B-B section in Figs. 3-4(e)-4(h)). After placing all the PCMs on the CP the production of the BRB are completed (Fig. 4(l)) and then the BRB is removed from the frame system in order to fix that into the test setup (Fig. 4(m)).

Table 1 Experimental program

| Specimen No | CM Details | PCM Dim.* (cm) /nbr of PCMs** | Gap*** (mm) | CP Yield Strength (MPa) | Concrete Strength (MPa) | Pe/Py | Reinf. of PCM | Anchorage Rod of PCM | |
|---|---|---|---|---|---|---|---|---|---|
| | | | | | | | | Nbr | Dia. |
| BRB1 | PCM | 17x17/14 | 4 | 330 | 21.5 | 2.8 | - | 4 | ϕ8 |
| BRB2 | PCM | 17x17/14 | 4 | 330 | 25.4 | 3.3 | ϕ8 | 4 | ϕ10 |
| BRB3 | PCM | 17x17/14 | 4 | 330 | 26.3 | 3.5 | ϕ8 | 8 | ϕ 10 |
| BRB4 | PCM | 17x17/14 | 4 | 330 | 22.9 | 3.0 | ϕ8 | 16 | ϕ 12 |
| BRB5 | PCM | 19x19/18 | 4 | 250 | 21.3 | 5.8 | ϕ14 | 16 | ϕ 24 |
| BRB6 | PCM | 19x19/18 | 2 | 300 | 24.6 | 5.6 | ϕ14 | 16 | ϕ 24 |
| BRB7 | PCM+FRP | 19x19/18 | 2 | 300 | 23.7 | 5.4 | ϕ14 | 16 | ϕ 24 |

* Dimensions of PCMs; ** Number of PCMs; *** Gap between CP and CM

BRB2: This BRB was similar to BRB1. The main difference between BRB1 and BRB2 was the reinforcement used in the PCMs (Figs. 5(a)-5(d)). Due to brittle behavior of plain concrete used for the BRB1, ϕ8 reinforcement bars was added into the PCMs (Fig. 5(c)) for the BRB2.

BRB3: This BRB was similar to BRB2. The number and diameter of the longitudinal anchorage rods were increased for the BRB3 because of the global buckling of CM. The number and the diameter of longitudinal anchorage rods were increased from 4 to 8 and from 8 mm to 10 mm for the BRB3, respectively (Figs. 5(e)-5(h)).

BRB4: This BRB was similar to BRB3. The number and the diameter of the longitudinal anchorage rods were increased for the BRB4 because of the global buckling of CM.

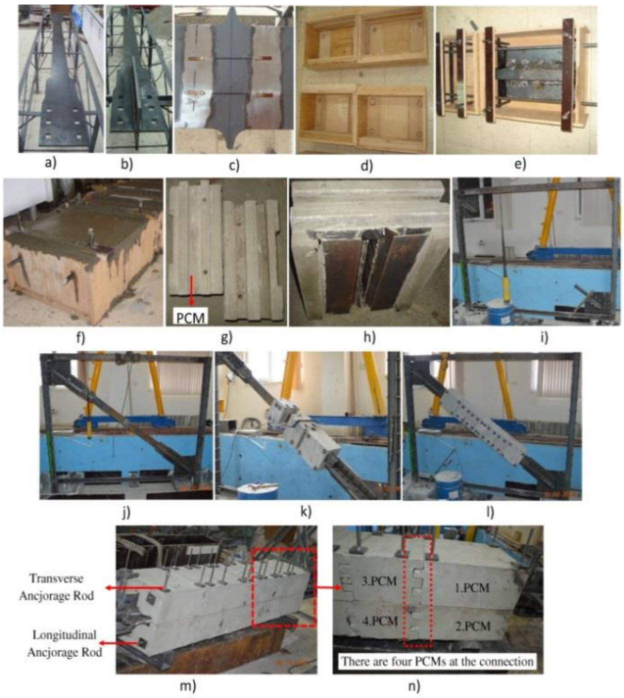


Fig. 4 Details of test specimens BRB1

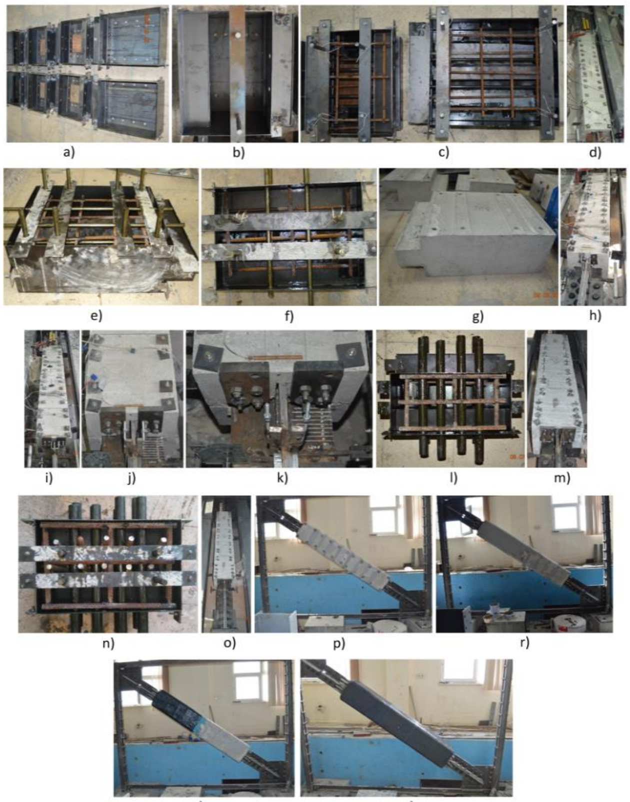


Fig. 5 Details of test specimens BRB2 to 7(a-d: BRB2, e-h: BRB3, i-k: BRB4, l-m: BRB5, n-o: BRB6, p-t: BRB7)

The number and the diameter of the longitudinal anchorage rods were increased from 8 to 16 and from 10 mm to 12 mm for the BRB4, respectively (Figs. 5(i)-5(k)). In addition, ϕ8 reinforcement rods were used in the perpendicular direction of PCMs.

BRB5: This BRB was similar to BRB4 except the cross-sectional area of PCMs and the diameter of reinforcements and longitudinal anchorage rods. The CM consisted of a 190 x 190 mm PCMs (Table 1 and Fig. 3). The diameter of the reinforcements and longitudinal anchorage rods were increased from 8 to 14 and from 12 to 24 for the BRB5, respectively (Figs. 5(l)-(m)). Furthermore, an additional connection was provided by using repair mortar between PCMs. In addition, the post-tensioning force about 75 kN was applied to each longitudinal anchorage rods. This force produced about 35% axial load ratio (ratio between applied total force and PCM axial load capacity) on the PCMs.

BRB6: This BRB was similar to the BRB5 except gap between CP and CM. It was 4 mm for the BRB5 and 2 mm for BRB6 (Table 1). In addition, the number of the reinforcement rods was increased and they placed on both surfaces of the PCMs (Figs. 5(n)-5(o)).

BRB7: This BRB was similar to BRB6. The FRP was wrapped on the PCMs instead of vertical anchorage rods. Three layers of FRP were used to wrap the PCMs. The BRB was placed in the steel frame as the other BRBs (Fig. 5(p)). After the repair putty was applied on the surface of the PCMs, the FRP was wrapped on the PCMs by using epoxy (Figs. 5(r)-5(s)). In order to prevent the FRP damage the corner of the PCMs were rounded. Finally, horizontal anchorage rods were fastened (Fig. 5(t)).

### *2.2 Instrumentation and loading system*

Fig. 6 indicates the test setup of loading system. The test setup was placed parallel to the ground and was a self-contained test setup system which carried the force by itself. The displacement and strain values on the test specimens were monitored by using a data acquisition system. The instrumentation details of the test specimens and the channel number (CN) of the data acquisition system from 1 to 19 are shown in Fig. 7. A displacement-controlled hydraulic piston with a capacity of 1000 kN was used to apply the axil force to the BRBs. A 1000-kN load cell (CN 1 in Fig. 7) located between the actuators and BRB was used to measure the axial load. In order to measure the axial displacement five Linear Variable Differential Transducers (LVDTs) were placed on the BRBs (CN 2–6 in Fig. 7). Due to slip-critical connection, the slip between the plates used to connect the BRB and gusset plate was also monitored from the LVDTs (CN 7–10 in Fig. 7) during the test. Furthermore, the LVDTs (CN 11–15 in Fig. 7) were used in order to measure the vertical and horizontal out-of-plane displacement of the BRB. An incremental quasi-static loading protocol was applied on the test specimens (Eryasar and Topkaya 2010, Tremblay *et al.* 2006, Iwata and Kato (2000). Two cycles were applied for each displacement defined in the testing protocol during the cyclic test. The loading protocol was as follows: $1/3\delta_y$, $2/3\delta_y$, $1.0\delta_y$, $1/3\delta_{str}$, $0.5\delta_{str}$, $1.0\delta_{str}$, $1.5\delta_{str}$, $2.0\delta_{str}$, $2.5\delta_{str}$, and $3.0\delta_{str}$, where $\delta_y$ and $\delta_{str}$ were the yield axial displacement and displacement value at 1.0% strain of the CP, respectively. As required in the AISC Seismic Provisions (2010) this loading protocol satisfies the cumulative axial deformation levels in excess of 200 times the yield displacement. For all experiments the cyclic loading started with compression excursion. The axial displacement demand was not applied to the center of the BRB hence an eccentricity was used during the test to impose rotation on the BRBs suggested by the AISC Seismic Provisions (2010).

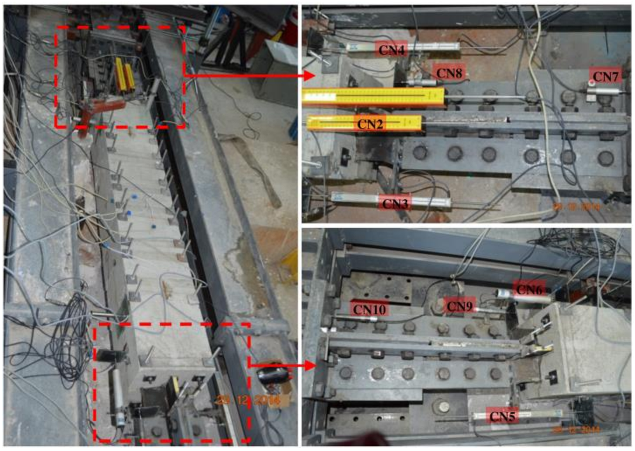


Fig. 6 Test setup of the loading system

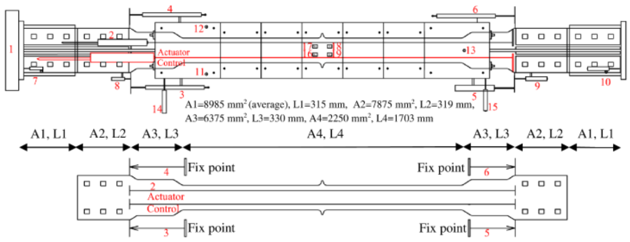


Fig. 7 Instrumentation of test members

## 3. Test results

Figs. 8 and 9 indicate the cyclic responses of the test specimens. In these figures, the test results are presented in terms of the axial strain of the CP versus applied axial force. As seen in Fig. 7 the value of axial strain of the CP was determined from the LVDTs (CN 2–6). Therefore, the average displacement of the LVDTs (CN 2–6) was divided by the length of the plastic part (1703 mm) of the CP (Fig. 7). This included the elastic displacement of the CP, but its effect is negligible. Fig. 10 indicates the pictures of the test specimens after testing. This figure also presents exaggerated drawings of the damage to the CP with a scale of 5 times. Table 2 presents the maximum and minimum axial forces measured during each test. This table also shows the compression strength adjustment factor, β, and the strain hardening adjustment factor, ω. The values of β and ω were calculated as averages for each strain cycle. Table 3 indicates the dissipated energy, dissipated energy normalized by the yield strength of the CP, and the tension and compression stiffness normalized by the theoretical stiffness values determined from the areas and length of the BRBs given in Fig. 7. The dissipated energy was calculated up to a CP strain of 2.0%. Tension and compression stiffness values were calculated at $(1/3)\delta_y$, $(2/3)\delta_y$, and $(1.0)\delta_y$. The maximum horizontal and vertical out-of-plane displacement and slip between plates used to connect the

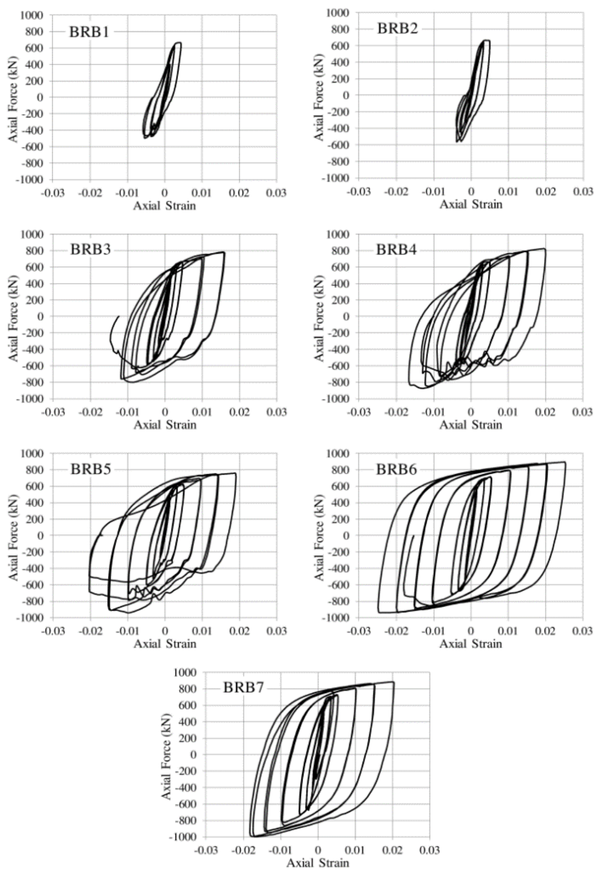


Fig. 8 Cyclic behavior of test specimens BRB1 to 7

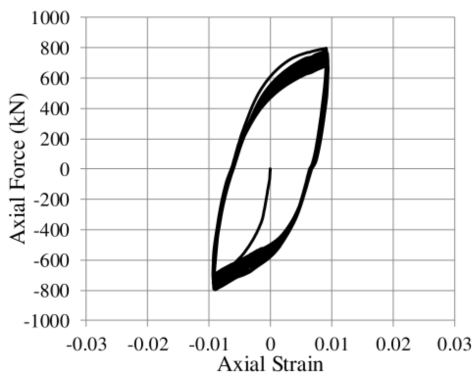


Fig. 9 Fatigue test of specimen BRB7

BRB and gusset plate are shown in Table 4 (Fig. 7 presents their CNs).

The specimen BRB1 showed unstable cyclic performance because of global buckling of the CM and significant local damage of the PCMs at the both ends (Figs. 8-10). While the former resulted from the insufficient longitudinal anchorage rods (Figs. 3 and 4(m)) the latter was due to plain concrete used for the PCMs had brittle behavior. There were four PCMs for each connection on the CP (Fig. 4(n)) and they were not completely pin or rigid. Hence the bending of the CM occurred at this location (Fig. 4(n)). Due to significant damage on the test specimen after CP strain of 0.5 % the further excursion was not applied to prevent the damage on the test setup and instrumentation. The axial compression capacity reached −497 kN during this test.

The specimen BRB2 had unstable cyclic performance due to significant damage on the CM (Fig. 10). Although the reinforcement was added to the PCMs (Fig. 5(c)), the local damage on the PCMs and global buckling of CM occurred. It was observed that the longitudinal anchorage rod (4-ϕ8) and the numbers of reinforcement (Fig. 5(c)) were not capable of providing sufficient strength and stability for the CM. The axial compression capacity reached −565 kN during this test. The test results of the specimens BRB1 and BRB2 indicated that the number of the longitudinal anchorage rods should be increased as well as the reinforcement placed into the PCMs. In fact, the pre-tension force of the longitudinal anchorage rods was found to be insufficient and this force should be increased. Therefore, it was planned to increase the number of longitudinal anchorage rods in the other BRB specimens.

The specimen BRB3 had more stable cyclic performance than the BRB1 and BRB2 as seen in Fig. 8. The higher numbers of the longitudinal anchorage rods (8-ϕ10) and reinforcement placed into the PCMs (Figs. 3-5) provided larger axial force capacity as -802 kN. In other words, the BRB3 had stable cyclic performance up to a CP strain of 1.0%. On the other hand, the damage initiated on the PCMs (Fig. 10) and then the axial force capacity dropped after the CP strain of 1.1%. Therefore, the test was stopped above the CP strain of 1.5% (Fig. 8). Although the numbers of the additional longitudinal anchorage rods (8-ϕ10) increased they seemed to be affective up to the CP strain of 1.0%. They could not fully control global buckling after CP strain of 1.0%. The local damage of CP accumulated on the first PCM of both ends of the BRB3 (Fig. 10).

The specimen BRB4 had more stable cyclic performance than the previous experiments as seen in Fig. 8. The 16-ϕ12 for the longitudinal anchorage rods and reinforcement placed into the PCMs (Figs. 3-5) provided larger axial force capacity as -876 kN. In fact, the damage occurred on the PCMs (Fig. 10) and then the axial force capacity dropped after the CP strain of 1.5%. This test indicated that the flexure capacity of the PCMs at each location of the connection needs to be strengthened.

The specimen BRB5 had more stable cyclic performance than the BRB4 (Fig. 8). There were initial cracks on the PCMs up to CP strain of 1.0%. Then, the cracks widened after the CP strain of 1.5% and then the local damage occurred at the second line of the PCMs (Fig. 10). The CP had significant local buckling at this location and the compression capacity of the BRB5 dropped after the CP strain of 1.5%. As it is seen from this experiment, the 16-ϕ24 for the longitudinal anchorage rods, additional reinforcement placed into the PCMs (Figs. 3-5) and higher cross-section of the PCMs resulted in larger CP strain and axial force capacity as -940 kN. Furthermore, the post-tensioning force and higher $P_e/P_y$ ratio (Table 1) enabled the BRB to sustain larger CP strain. On the other hand, the


Fig. 10 Physical damage of the specimens BRB1 to 7.

local damage on the CP (Fig. 10) indicated that the gap between CP and PCMs needs to be decreased.

The specimen BRB6 had a very stable cyclic performance up to a CP strain of 2.0% (Fig. 8). Furthermore, the behavior was also stable at the first cycle of the CP strain of 2.5% on the other hand the damage occurred on the PCMs at the second cycle of that strain in compression. Although the horizontal and vertical out-off-plane displacements in the PCMs were about 8-10 mm (Table 4), they did not affect the cyclic performance of the BRB6 (Fig. 8). The axial compression capacity reached −939 kN during this test. Although the high-mode buckling has occurred along the plastic zone on the CP, the local damage on the PCMs was seen due to the high amplitude of the buckling (Fig. 10). This behavior indicated that the PCMs need further confinement in order to resist the local or high mode buckling of the CP.

The cyclic performance of the specimen BRB7 was stable up to a CP strain of 2.0 % (Fig. 8). This specimen could not be loaded further due to the load cell capacity which was 1000kN. There was no damage on the test specimen at the end of the test. Hence, the fatigue test was applied to the specimen BRB7 (Fig. 9). During the fatigue test, 40 cycles were applied to the specimen at the CP strain of 1.0%. Even though no damage was observed on the BRB7, the fatigue test was stopped after 40 cycles. After

Table 2 Maximum and minimum axial forces and ω and β factors

| Specimen No | Max. Axial Force (kN) | | Force Ratio *** | ω and β factors | | | | | | | | | |
|---|---|---|---|---|---|---|---|---|---|---|---|---|---|
| | | | | 0.33% | | 0.50% | | 1.00% | | 1.50% | | 2.00% | |
| | T* | C** | | ω | β | ω | β | ω | β | ω | β | ω | β |
| BRB1 | 666 | -497 | 0.75 | 1.004 | 0.744 | NA | NA | NA | NA | NA | NA | NA | NA |
| BRB2 | 665 | -565 | 0.85 | 1.000 | 0.710 | NA | NA | NA | NA | NA | NA | NA | NA |
| BRB3 | 784 | -802 | 1.02 | 1.004 | 0.842 | 1.055 | 0.884 | 1.142 | 0.926 | 1.235 | 0.974 | NA | NA |
| BRB4 | 825 | -876 | 1.06 | 1.002 | 0.840 | 1.038 | 0.902 | 1.141 | 0.997 | 1.235 | 1.038 | NA | NA |
| BRB5 | 758 | -940 | 1.24 | 1.005 | 0.842 | 1.037 | 0.971 | 1.139 | 1.094 | 1.242 | 1.241 | NA | NA |
| BRB6 | 895 | -939 | 1.05 | 1.002 | 0.972 | 1.042 | 1.003 | 1.159 | 1.041 | 1.227 | 1.061 | 1.269 | 1.072 |
| BRB7 | 887 | -1002 | 1.13 | 1.001 | 0.949 | 1.039 | 1.002 | 1.155 | 1.044 | 1.225 | 1.100 | 1.185 | 1.205 |

* Tension force; ** Compression force; *** Force ratio of tension and compression force

Table 3 Dissipated energy and normalized stiffness value

| Specimen | Dissipated Energy (kN mm) | Normalized Dissipated Energy | Compression and Tension Normalized Stiffness Values | | | | | |
|---|---|---|---|---|---|---|---|---|
| | | | Compression Stiffness | | | Tension Stiffness | | |
| | | | δy/3 | 2δy/3 | δy | δy/3 | 2δy/3 | δy |
| BRB1 | 17118 | 23 | 0.779 | 0.719 | 0.670 | 0.885 | 0.831 | 0.790 |
| BRB2 | 16919 | 23 | 0.784 | 0.662 | 0.605 | 1.043 | 0.925 | 0.850 |
| BRB3 | 177365 | 239 | 0.930 | 0.773 | 0.640 | 1.089 | 0.959 | 0.899 |
| BRB4 | 242249 | 326 | 0.726 | 0.646 | 0.651 | 1.133 | 1.028 | 0.940 |
| BRB5 | 281078 | 500 | 0.743 | 0.713 | 0.604 | 1.251 | 1.073 | 0.998 |
| BRB6 | 391356 | 580 | 1.142 | 1.068 | 1.027 | 1.149 | 1.080 | 1.033 |
| BRB7 | 354783 | 526 | 0.990 | 0.899 | 0.872 | 1.060 | 1.017 | 0.992 |

removing the CP from the CM or PCMs, the minor cracks at the end of the PCMs and the minor local buckling of the CP was observed (Fig. 10). It was observed that the further damage of the PCMs was prevented by FRP wrapped round it. In fact, the local buckling of the CP resulted in the cracks on the PCMs but the FRP provided the confinement effect for them to prevent the further damage. Hence, the application of the FRP was found to be a very effective in sustaining the stability of PCMs. Furthermore, the horizontal and vertical out-off-plane displacements in the CM were about 20-40 mm (Table 4) but they did not affect the cyclic performance of the BRB7 (Fig. 8).

## 4. Discussion of test results

The test results indicated that the cyclic performances of BRB6 and 7 seemed to be acceptable. As it can be seen in Table 2, the compression strength adjustment factor, β, of these BRBs is lower than the limit of 1.3 given by the AISC Seismic Provisions (2010). The main reason of this result was the amount of friction, which dominates β, eliminated as far as possible by using 2-mm air gap for each surface of the CP. On the other hand, the 4mm gap between the CM and the CP was found to be large for specimen BRB1-5. This large gap was observed to be one of the reasons of the local damage of the CP. The nominal yield strength of the CP was 235 MPa (S235 given in Turkish Steel Design Code 2016) for all BRBs. On the other hand, the coupon tests indicated that the yield strength of the CP was generally higher than 235 MPa given in Table 1. As a result, the mechanical properties of the CP should be determined before the design of any BRB braced system. The value of the strain hardening adjustment factor, ω, was found between 1.14-1.16 for all BRBs (Table 2). This is because of the main parameters that affect the value of ω such as steel properties, loading, and BRB details. As seen in Table 3, the energy dissipation capacity and the normalized dissipated energy of BRB6 and 7 were the highest among the tested BRBs up to a CP strain of 2.0%. It was found from the test results that the energy dissipation capacity of the BRBs depended significantly on the stability of the PCMs. The theoretical stiffness of the BRBs was determined to be 240, 219, and 204 kN/mm for the areas and lengths of (A4, L4 + A3, L3), (A4, L4 + A3, L3 + A2, L2), and (A4, L4 + A3, L3 + A2, L2 + A1, L1), as shown in Fig. 7, respectively. Table 3 indicates the values of tension and compression stiffness of the BRBs normalized with the theoretical stiffness as 204 kN/mm. In fact, they were calculated at $1/3\delta_y$, $2/3\delta_y$, and $1.0\delta_y$ in this table.

Table 4 Maximum horizontal and vertical out-of-plane displacement and slip between plates used to connect the BRB and gusset plate (The channel numbers are given in Fig. 7)

| Specimens | Slip (mm) | | | | Vertical Displ. (mm) | | Horizontal Displ. (mm) | | |
|---|---|---|---|---|---|---|---|---|---|
| | CN7 | CN8 | CN9 | CN10 | CN11 | CN12 | CN13 | CN14 | CN15 |
| BRB1 | 0.1 | 0.1 | 0.1 | 0.0 | 18.3 | 3.6 | 10.1 | 3.1 | 3.4 |
| | 0.0 | 0.0 | -0.2 | 0.0 | -7.6 | -24.4 | -3.1 | -11.2 | -1.2 |
| BRB2 | 0.2 | 0.1 | 0.1 | 0.0 | 0.6 | 1.8 | 0.3 | 1.0 | 22.0 |
| | -0.2 | -0.1 | -0.2 | -0.1 | -18.3 | -11.0 | -2.9 | -1.4 | -0.6 |
| BRB3 | 0.5 | 0.1 | 0.1 | 5.9 | 5.9 | 25.3 | 5.9 | 3.7 | 3.0 |
| | -0.2 | -0.1 | -1.6 | -3.1 | -2.1 | -64.6 | -2.7 | -1.1 | -7.6 |
| BRB4 | 0.2 | 0.1 | 0.1 | 0.0 | 2.9 | 1.2 | 2.5 | 2.1 | 1.9 |
| | -0.1 | -0.1 | -0.1 | 0.0 | -4.4 | -3.0 | -0.2 | -4.2 | -4.2 |
| BRB5 | 0.2 | 0.0 | 0.1 | 0.1 | 7.0 | 6.0 | 6.7 | 7.8 | 1.3 |
| | -0.1 | -0.1 | -0.1 | -0.1 | -1.2 | -4.3 | -6.1 | -6.8 | -1.7 |
| BRB6 | 0.4 | 0.1 | 0.1 | 0.0 | 10.0 | 2.2 | 4.2 | 8.0 | 1.1 |
| | -0.1 | -0.1 | -0.1 | -0.1 | -0.1 | -5.7 | -4.1 | -4.4 | -2.5 |
| BRB7 | 0.3 | 0.1 | 0.1 | 0.1 | 38.8 | 5.8 | 6.2 | 24.3 | 0.8 |
| | -0.3 | 0.0 | -0.1 | -0.1 | -8.1 | -38.7 | -3.0 | -2.8 | -2.6 |

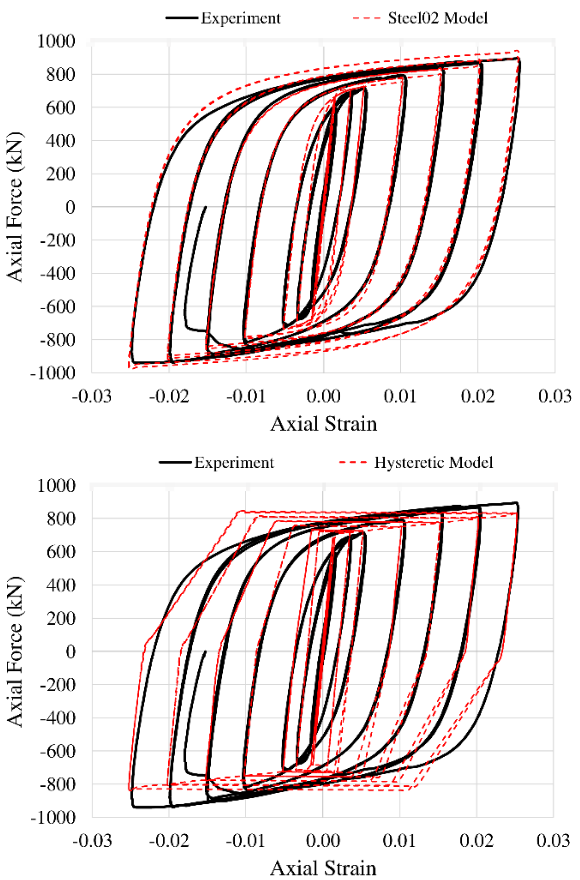


Fig. 11 Simulation of cyclic behavior of the test specimen BRB6 with Steel02 and Hysteretic material models

It was determined from Table 3 that the values of tension and compression stiffness in the cycle of $1/3\delta_y$ are usually higher than in the cycles of $2/3\delta_y$ and $1.0\delta_y$. The global buckling of the CM was seemed to have effect on the compression stiffness of the BRBs. Furthermore, it was found from the test results that the friction between CP and PCMs and initial loading started with compression excursion dominated the initial stiffness of the BRBs.

In addition, the stiffness of the BRBs may be affected by the slip between the gusset plate and the CP. Table 4 indicates the value of the slip may increase to an important amount for some of the specimens. Although the workmanship and equipment used for the connection were almost same, the slip can't be prevented. Hence, it may be appropriate to include this slip during the design of the BRB braced frames. Table 4 also indicates the vertical and horizontal out-of-plane displacements measured at the both ends of the BRBs (channels from CN11 to CN15, Fig. 7). Although these displacements of BRB6 and 7 were between 10 and 40 mm, the cyclic responses of these BRBs were stable (Table 3 and Fig. 8). This means that using the reinforcement in the PCMs, increasing the number and diameter of the anchorage rods, decreasing the air gap between the CP and CM, and the PCMs wrapped with FRP provided the BRB6 and 7 to sustain stable hysteretic behavior.

## 5. Analytical study

An analytic study was performed to verify the test results in terms of cyclic behavior. The test specimen BRB6 was modelled by utilizing the OpenSees simulation platform (Mazzoni *et al.* 2009). As shown in Figs. 1-7, the test specimen was modelled as single member with elastic and plastic parts. The plastic and elastic zones of the BRB were modelled as truss member and elastic Beam Column, respectively. The testing protocol, used for the analytical BRB model, was same as that applied for the test specimens. Two material models namely Hysteretic and Steel02 were used in order to simulate the test specimen accurately (Ozcelik *et al.* 2017). The Hysteretic material model can be used to construct a uniaxial bilinear hysteretic material object with pinchX (pinching factor for strain during reloading), pinchY (pinching factor for stress during reloading), damage1 (ductility-based damage accumulation), and damage2 (damage due to energy) (Mazzoni *et al.* 2009). The Steel02 material model can be used to construct a uniaxial steel material object with isotropic strain hardening. Further details of the Hysteretic and Steel02 material model can be found at Mazzoni *et al.* (2009). Fig. 11 indicates that the Steel02 material model simulated the cyclic behavior of test specimen BRB6 better than Hysteretic material model. As a result, the BRBs in a braced frame can be modelled with an acceptable accuracy by using Steel02 material model.

## 6. Conclusions

Seven full-scale BRB specimens were tested in this study. The cyclic response of the BRBs with various design parameters were determined. The new designed BRBs were aimed to construct inside the existing deficient structures for the retrofitting solution since the PCMs can placed on the CP step by step. The weight of the PCMs was between 40 and 60 kg which can be carried without using a forklift or other devices. The plain and reinforced concrete and reinforced concrete wrapped with FRP were used for the CMs. The following conclusions can be drawn based on the observed responses of the test specimens:

- The cyclic performance and stability of the BRBs is significantly dependent on the CM.
- The plain concrete which has at least 20MPa compressive strength as a CM was found incapable for providing sufficient capacity and stability due to brittle failure.
- The usage of reinforcement in the PCMs postponed the damage of CM and enabled the CP to maintain larger CP strain up to 2.0%. In fact, the major local damage of the PCMs was prevented by using the FRP provided confinement effect. Furthermore, the numbers, diameter and post-tensioning force of the longitudinal anchorage rods dominated to the global stability of the CM. The level of post-tensioning force mentioned as axial load ratio (about 35%) was seen sufficient to prevent the global buckling. In addition, the ratio of $P_e/P_y$ which was between 2.8 and 5.8 has also effect on it. The value of $P_e/P_y$ ratio was found to be at least 5.0 for the PCMs in this study.
- The slip measured between the gusset plate and the CP may result in decreasing the axial stiffness of BRB hence it needs to be included during the design of the BRB braced frame.
- The compression strength adjustment factor, β, is significantly dependent on the isolation between the CM and the CP. Therefore, the 2 mm air gap seemed to provide sufficient isolation between the CM and CP with respect to the test results.
- It was found from the test results that the energy dissipation capacity of the BRBs was significantly dependent on the stability of the CM in addition to values of β and ω. In fact, the increment of the β, ω, post-tensioning force and $P_e/P_y$ triggered the energy dissipation capacity of the BRBs.
- As a result of this study, the design methodology of the specimens BRB6 and BRB7 capable of sustaining 2.0% CP strain was seen to be successful with respect to test results.

## Acknowledgments

The research discussed in this paper was conducted at Akdeniz University Structural Mechanics Laboratory. Funding provided by TUBITAK [grant number: 112M820] is greatly appreciated. Also, the authors thank Professor Baris Binici and Professor Cem Topkaya (from METU) for their contributions to this study.

## References

AISC (2010), Seismic provisions for structural steel buildings, American Institute of Steel Construction Ins.

Avci, C., Celik, O.C. and Yalcin, C. (2018), "Experimental investigation of aluminum alloy and steel core buckling restrained braces (BRBs)", *Int. J. Steel Struct.*, **18**(2), 650-673. https://doi.org/10.1007/s13296-018-0025-y.

Beiraghi, H. (2017), "Earthquake effects on the energy demand of tall reinforced concrete walls with buckling-restrained brace outriggers", *Struct. Eng. Mech.*, **63**(4), 521-536. https://doi.org/10.12989/sem.2017.63.4.521.

Beiraghi, H. (2018a), "Energy demands in reinforced concrete wall piers coupled by buckling restrained braces subjected to near-fault earthquake", *Steel Compos. Struct*., **27**(6), 703-716. https://doi.org/10.12989/scs.2018.27.6.703.

Beiraghi, H. (2018b), "Reinforced concrete core-walls connected by a bridge with buckling restrained braces subjected to seismic loads", *Earthq. Struct.*, **15**(2), 203-214, https://doi.org/10.12989/eas.2018.15.2.203.

Beiraghi, H. (2019), "Fragility assessment of shear walls coupled with buckling restrained braces subjected to near-field earthquakes", *Steel Compos. Struct*., **33**(3), 389-402, https://doi.org/10.12989/scs.2019.33.3.389.

Black, C., Aiken, I. and Makris, N. (2002), "Component testing, stability analysis and characterization of buckling-restrained unbonded braces", PEER Report 2002/08, University of California, California, USA.

Black, G., Wenger, W.A. and Popov, E.P. (1980), "Inelastic buckling of steel struts under cyclic load reversals", UCB/EERC-80/40, University of California, USA.

Brown, A.P., Aiken, I.D. and Jafarzadeh, F.J. (2001), "Seismic Retrofit of the Wallace F. Bennett Federal Building", *Mod. Steel Constr.*, **41**(8), 123-124.

Chen, C.C., Chen, S.Y. and Liaw, J.J. (2001), "Application of low yield strength steel on controlled plastification ductile concentrically braced frames", *Can. J. Civ. Eng.*, **28**(5), 823-836. https://doi.org/10.1139/l01-044.

Chou, C.C., Chung, P.T. and Cheng, Y.T. (2016), "Experimental evaluation of large-scale dual-core self-centering braces and sandwiched buckling-restrained braces'', *Eng. Struct*., **116**(1), 12-25. https://doi.org/10.1016/J.ENGSTRUCT.2016.02.030.

Christopulos, A.S. (2005), "Improved seismic performance of buckling restrained braced frames'', Ph.D. Dissertation, University of Washington, Washington.

DiSarno, L. and Elnashai, A.S. (2008), "Bracing systems for seismic retrofitting of steel frames'', *J. Constr. Steel Res*., **65**(2), 452-465. https://doi.org/10.1016/j.jcsr.2008.02.013.

DiSarno, L. and Manfredi, G. (2010), "Seismic retrofitting with buckling restrained braces: Application to an existing non-ductile RC framed building'', *Soil Dyn. Earthq. Eng.*, **30**(11), 1279-1297. https://doi.org/10.1016/j.soildyn.2010.06.001.

DiSarno, L. and Manfredi, G. (2012), "Experimental tests on full-scale RC unretrofitted frame and retrofitted with buckling-restrained braces'', *Earthq. Eng. Struct. D.*, **41**(2), 315-333. https://doi.org/10.1002/eqe.1131.

Eryasar, M.E. and Topkaya, C. (2010), "An experimental study on steel-encased buckling-restrained brace hysteretic dampers'', *Earthq. Eng. Struct. Dyn.*, **39**(5), 561-581. https://doi.org/10.1002/eqe.959.

Fahnestock, L.A., Ricles, J.M. and Sause, R. (2007), "Experimental evaluation of a large-scale buckling-restrained braced frame'', *J. Struct. Eng.*, **133** (9), 1205-1214. https://doi.org/10.1061/(ASCE)0733-9445(2007)133:9(1205).

Fujishita, K., Bal, A., Sutcu, F. and Celik, O.C., Takeuchi, T., Matsui, R. *et al.* (2015), "Comparing hysteretic behavior of buckling restrained braces (BRBs) with bolted and welded end connections'', *Proceedings of the 8th International Symp. Steel Struct.,* Jcju, Korea, November.

Haydaroglu, C., Taskin, K. and Celik, O.C. (2011), "Ductility enhancement of round HSS braces using CFRP sheet wraps'', *Proceedings of the 6th Eur. Conf. Steel Compos. Struct*., Budapest, Hungary, September. https://doi.org/10.13140/2.1.1299.4246.

Higgins, C.C. and Newell, J.D. (2004), "Confined steel brace for earthquake resistant design'', *Eng. J. AISC.*, **41**(4), 187–202.

Hikino, T., Okazaki, T., Kajiwara, K. and Nakashima, M. (2011), "Out-of-plane stability of buckling-restrained braces'', *Proceeding of the Structures Congres*., Nevada, USA, April. https://doi.org/10.1061/41171(401)83.

Hikino, T., Okazaki, T., Kajiwara, K. and Nakashima, M. (2013), "Out-of-plane stability of buckling-restrained braces placed in chevron arrangement'', *J. Struct. Eng.*, **139**(11), 1812-1822. https://doi.org/10.1061/(ASCE)ST.1943-541X.0000767.

Iwata, M. and Kato. T. (2000), "Buckling-restrained braces as hysteretic dampers'', *Proceedings of the Int. Conf. 3rd, Behav. Steel Struct. Seism. Areas*, Montreal, Canada.

Kasai, K., Ooki, Y., Ishii, M., Ozaki, H., Ito, H. and Motoyui, S. (2008), "Value-added 5-story steel frame and its components: Part 1—Full-scale damper tests and analyses'', *Proceedings of the 14th World Conf. Earthq. Eng.,* Beijing, China, October.

Kim, J., Choi, H. and Chung, L. (2004), "Energy-based seismic design of structures with buckling-restrained braces'', *Steel Compos. Struct.*, **4**(6), 437-452. https://doi.org/10.12989/scs.2004.4.6.437.

Li, Y., Qu, H., Xiao, S., Wang, P., You, Y. and Hu, S. (2019). "Behavior of three-tube buckling-restrained brace with circumference pre-stress in core tube'' *Steel Compos. Struct*., **30**(2), 81-96. https://doi.org/10.12989/scs.2014.16.5.491.

Lin, M., Tsai, K., Hsiao, P. and Tsai, C. (2005), "Compressive behavior of buckling-restrained brace gusset connections'', *Proceedings of the 1st Int. Conf. Adv. Exp. Struct. Eng. AESE*, Nagoya, Japan, July.

Lin, M.L., Tsai, K.C. and Tsai, C.Y. (2006), "Bi-directional sub-structural pseudo-dynamic tests of a full-scale 2-story BRBF, Part 2 : Compressive behavior of gusset plates'', *Proceedings of the 8th U. S. Natl. Conf. Earthq. Eng*., San Francisco, USA.

Lopez, W.A., Gwie, D.S., Lauck, T.W. and Saunders, C.M. (2004), "Structural design and experimental verification of a buckling-restrained braced frame system'', *Eng. J. AISC.*, **41**(4), 177-186.

Maalek, S., Heidary-Torkamani, H., Pirooz, M.D. and Naeeini, S.T.O. (2019)." Numerical investigation of cyclic performance of frames equipped with tube-in-tube buckling restrained braces'', *Steel Compos. Struct*., **30**(3), 201-215. https://doi.org/10.12989/scs.2019.30.3.201.

Mazzolani, F.M.M. (2008), "Innovative metal systems for seismic upgrading of RC structures'', *J. Constr. Steel Res*., **64**(7), 882-95, https://doi.org/10.1016/j.jcsr.2007.12.017.

Mazzoni S., McKenna F., Scott M.H. and Fenves G.L. (2009), Open system for earthquake engineering simulation (OpenSees), User command language manual, Pacific Earthquake Engineering Research Center, University of California, Berkeley, CA, USA.

Merritt, S., Uang, C.M. and Benzoni, G. (2003), "Subassemblage testing of star seismic buckling-restrained braces'', Report no TR-2003/04, San Diego, University of California.

Mirtaheri, S.M., Nazeryan, M., Bahrani, M.K., Nooralizadeh, A., Montazerian, L. and Naserifard, M. (2017), "Local and global buckling condition of all-steel buckling restrained braces'', *Steel Compos. Struct.*, **23**(2), 217-228. https://doi.org/10.12989/scs.2017.23.2.217.

Ozcelik, R., Binici, B. and Kurç, O. (2012), "Pseudo Dynamic Testing of an RC Frame Retrofitted with Chevron Braces'', *J. Earthq. Eng.*, **16**(4), 515-539. http://dx.doi.org/10.1080/13632469.2011.653297.

Ozcelik, R. and Erdil, E.F. (2019), "Pseudo dynamic test of a deficient RC frame strengthened with buckling restrained braces'', *Earthq. Spectra,* **35**(3), 1163-1187. https://doi.org/10.1193/122317EQS263M.

Ozcelik, R., Dikiciasik, Y. and Erdil, E.F. (2017), "The development of the buckling restrained braces with new end restrains'', *J. Constr. Steel Res.*, **138**(1), 208-220. https://doi.org/10.1016/j.jcsr.2017.07.008.

Pandikkadavath, S.M. and Sahoo, R.D. (2016), "Analytical investigation on cyclic response of buckling-restrained braces with short yielding core segments'', *Int. J. Steel Struct*., **16**(4), 1273–85. https://doi.org/10.1007/s13296-016-0083-y.

Park, J., Lee, J. and Kim, J. (2012), "Cyclic test of buckling restrained braces composed of square steel rods and steel tube'', *Steel Compos. Struct.*, **13**(5), 423-436. https://doi.org/10.12989/scs.2012.13.5.423.

Razavi, S.A., Kianmehr, A., Hosseini, A. and Mirghaderi, S.R. (2018). "Buckling-restrained brace with CFRP encasing: Mechanical behavior & cyclic response'', *Steel Compos. Struct.,* **27**(6), 675-689. https://doi.org/10.12989/scs.2018.27.6.675.

Sabelli, R., Mahin, S. and Chang, C. (2003), "Seismic demands on steel braced frame buildings with buckling-restrained braces'', *Eng. Struct.,* **25**(5), 655-666, https://doi.org/10.1016/S0141-0296(02)00175-X.

Sherman, J. and Okazaki, T. (2010), "Bidirectional loading behavior of buckling-restrained braced frames'', *Proceedings of the Structures Congress*, Orlando, Florida, USA, May. https://doi.org/10.1061/41130(369)320.

Sutcu, F., Takeuchi, T. and Matsui, R. (2014), "Seismic retrofit design method for RC buildings using buckling-restrained braces and steel frames'', *J. Constr. Steel. Res.*, **101**(1), 304-313. https://doi.org/10.1016/j.jcsr.2014.05.023.

Takeuchi, T., Hajjar, J.F., Matsui, R., Nishimoto, K. and Aiken, I.D. (2012), "Effect of local buckling core plate restraint in buckling restrained braces'', *Eng Struct*, **44**(1), 304-311. https://doi.org/10.1016/J.ENGSTRUCT.2012.05.026.

Takeuchi, T., Ida, M., Yamada, S. and Suzuki, K. (2008), "Estimation of cumulative deformation capacity of buckling restrained braces”, *J. Struct. Eng.,* **134**(5), 822-831, https://doi.org/10.1061/(ASCE)0733-9445(2008)134:5(822).

Takeuchi, T., Ozaki, H., Matsui, R. and Sutcu, F. (2014), “Out-of-plane stability of buckling-restrained braces including moment transfer capacity”, *Earthq. Eng. Struct. D*., **43**(6), 851-869. https://doi.org/10.1002/eqe.2376.

Tremblay, R., Bolduc, P., Neville, R. and DeVall, R. (2006), “Seismic testing and performance of buckling-restrained bracing systems”, *Can. J. Civ. Eng.*, **33**(2), 183-198. https://doi.org/10.1139/l05-103.

Tsai, K., Lai, J., Hwang, Y., Lin, S. and Weng, C. (2004), “Research and application of double-core buckling restrained braces in Taiwan”, *Proceedings of the 13th World Conference on Earthquake Engineering*, Vancouver, Canada, August.

Tsai, K.C. and Hsiao, P.C. (2008), “Pseudo-dynamic test of a full-scale CFT/BRB frame-Part II: Seismic performance of buckling-restrained braces and connections”, *Earthq. Eng. Struct. D.,* **37**(7), 1099-1115. https://doi.org/10.1002/eqe.803.

Tsai, K.C., Hsiao, P.C., Wang, K.J., Weng, Y.T., Lin, M.L., Lin, K.C. *et al.* (2008), “Pseudo-dynamic tests of a full-scale CFT/BRB frame-Part I: Specimen design, experiment and analysis”, *Earthq. Eng. Struct. D.*, **37**(7), 1081-1098. https://doi.org/10.1002/eqe.804.

Tsai, K.C., Hwang, Y.C., Weng, C.S., Shirai, T. and Nakamura, H. (2002), “Experimental tests of large scale buckling restrained braces and frames”, *Proceedings of the Passiv. Control Symp*., Tokyo, Japan.

Tsai, K.C., Weng, Y.T., Wang, K.J., Tsai, C.Y. and Lai, J.W. (2006), “Bi-directional sub-structural pseudo-dynamic testing of a full scale 2-Story BRBF, Part 1: Seismic design, analytical and experimental performance assessments”, *Proceedings of the 8th U. S. Natl. Conf. Earthq. Eng*., San Francisco, USA.

Turkish Steel Design Code (2016), Design, calculation and construction details for steel structures, Ankara, Turkey. (In Turkish).

Uang, C.M. and Nakashima, M. (2004), Earthquake engineering : from engineering seismology to performance-based engineering, CRC Press, Florida, USA.

Uang, C.M., Nakashima, M. and Tsai, K.C. (2004), “Research and application of buckling-restrained braced frames”, *Int. J. Steel Struct.*, **4**(4), 301-313.

Uriz, P. (2005), “Towards earthquake resistant design of concentrically braced steel structures”, Ph.D. Dissertation, University of California, California.

Usami, T., Ge, H. and Kasai, A. (2008), “Overall buckling prevention condition of buckling-restrained braces as a structural control damper”, *Proceedings of the 14th World Conference on Earthquake Engineering,* Beijing, China, October.

Usami, T., Ge, H. and Luo, X. (2009), “Experimental and analytical study on high-performance buckling-restrained brace dampers for bridge engineering”, *Proceedings of the 3rd International Conf. AESE*, San Francisco, USA, October.

Usami, T., Wang, C.L. and Funayama, J. (2012), “Developing high-performance aluminum alloy buckling-restrained braces based on series of low-cycle fatigue tests”, *Earthq. Eng. Struct. D.*, **41**(4), 643-661. https://doi.org/10.1002/eqe.1149.

Wang, C.L., Usami, T., Funayama, J. and Imase, F. (2013), “Low-cycle fatigue testing of extruded aluminium alloy buckling-restrained braces”, *Eng. Struct.*, **46**(2), 94–301. https://doi.org/10.1016/J.ENGSTRUCT.2012.07.016.

Watanabe, A., Hitomi, Y., Saeki, E., Wada, A. and Fujimoto, M. (1988), “Properties of brace encased in buckling-restraining concrete and steel tube”, *Proceedings of the 9th World Conference on Earthquake Engineering*, Tokyo-Kyoto, Japan, August.

Xie, Q. (2004), “State of the art of buckling-restrained braces in Asia”, *J. Constr. Steel Res.*, **61**(6), 727-748. https://doi.org/10.1016/J.JCSR.2004.11.005.

Young, Y.K., Kim, M.H., Kim, J. and Kim, S.D. (2009), “Component tests of buckling-restrained braces with unconstrained length”, *Eng. Struct.*, **31**(2), 507-516, https://doi.org/10.1016/J.ENGSTRUCT.2008.09.014.

*CC*